Dicopper Cryptates with 1,1 and 1,3 Bridging Ligands: Spectroscopic, Magnetic and Electrochemical Properties†

Qin Lu,[a] Jean-Marc Latour,[b] Charles J. Harding,[c] Noreen Martin,[a] Debbie J. Marrs,[a,c] Vickie McKee*,[a] and Jane Nelson*,[a,c]

[a] Chemistry Department, Queens University, Belfast BT9 5AG, UK

[b] Laboratoire DRFMC/SESAM/CC, C.E.N.G., BP 85X 38041 Grenoble Cedex, France

[c] Chemistry Department, Open University, Milton Keynes MK7 6AA, UK

The furan-based hexaiminocryptand L^1, $N[(CH_2)_2N=CHRCH=N(CH_2)_2]_3N$ where R = furan-2,5-diyl, has been found to act as host for dicopper(I) and μ-hydroxo-dicopper(II). The corresponding octaaminocryptand derivative L^2 accommmodated dicopper(II) with hydroxide, imidazolate or azide bridging ligands. A single-crystal X-ray analysis of $[Cu_2L^1][BF_4]_2$ revealed trigonal-pyramidal co-ordination for Cu^I together with a Cu $\cdots$ Cu separation of 4.2 Å. The μ hydroxo-dicopper(II) cryptate $[Cu_2L^2(OH)][CF_3SO_3]_2$ was found to have trigonal-bipyramidal geometry, with a Cu $\cdots$ Cu separation of 3.9 Å and the Cu–OH–Cu assembly close to linear. Effective magnetic exchange arising from collinear disposition of bridge O $2p_z$ and copper(II) magnetic orbitals makes the hydroxo-bridged derivatives effectively diamagnetic.

Although it is over 15 years since the concept of 'cascade' complexation was elegantly formulated by Lehn[1] in the context of cryptand hosts, the development of suitable cryptand systems has been slow to follow. This tardiness may in part arise because of the labour involved in synthesising cryptands of appropriate donicity; the more familiar O-donor cryptands are poor hosts for the transition-metal cations which are required to form the bimetallic cryptate capable of hosting a bridging ligand.

The newly developed facile synthetic route to azacryptands[2,3] furnishes a series of sp^3 and sp^2 N-donor cryptands (Scheme 1), with tuneable distance between potential co-ordination sites; these are ideal precursors for the bimetallic cryptates needed to act as hosts for the bridges to be incorporated between a pair of cations. At present our effort is concentrated mainly on the more stable and easily characterisable complexes incorporating anionic bridging ligands, which permits the characterisation of preferred bridging geometry. Knowledge of the optimum parameters should then assist planning of strategy aimed at incorporation of the less strongly held, but possibly catalytically useful, bridging ligands. The investigation of a wide range of bridged cryptate systems may eventually result in the fulfilment of their potential[1] 'in relation to transport, catalysis or activation of the fixed substrate or as bioinorganic models for metalloproteins'.

Our earlier reports on bridged and unbridged dicopper cryptates have described[4-8] systems with internuclear distances ranging from ≈ 7 to 2.4 Å, containing copper in oxidation state +1 and/or +2, and exhibiting varying degrees of interaction between the copper cations, as demonstrated by magnetic and electrochemical behaviour. Many of the hexaimino cryptates are prone to hydrolytic breakdown, particularly when the cations are in oxidation state > 1, which hinders examination of solution properties of the dicopper(II) salts.[5,7,9] However, there were indications that the present hexaiminocryptand, L^1, had reasonable stability towards hydrolysis, so there seemed to be a good chance of isolating both dicopper-(I) and -(II) cryptates

and studying their solution properties. The octaamino derivative L^2, in common with other compounds of this type, presents no problem in respect of solution stability even when co-ordinated to Lewis acids, so the dicopper(II) cryptate may be expected to act as host for a wide range of bridging ligands.

The compound L^1, obtained in good yield by [2 + 3] condensation of tris(2-aminoethylamine) (tren) with 2,5-diformylfuran, has a divergent conformation[10] in the metal-free state, where only the bridgehead N-donors (separated by 10.4 Å) are directed into the 'cavity', which in fact is so tiny that it contains little free space and at first sight might seem capable of offering no more than meagre hospitality to guests. However, in the presence of suitable cations, the cryptand can be seen to adopt quite different conformations, with at least some of the imine donors directed convergently. This was first inferred in Group II cryptates from examination of ^1H NMR spectra[10,12] and has since been confirmed[12] by X-ray crystallography for the Group I cryptate, $[NaL^1]^+$. Except in the case of the barium complex, mononuclear cationic complexes are associated with complex ^1H NMR spectra[9] deriving from unsymmetric siting of the cation within the macrobicyclic cavity. However, the disilver cryptate[11] obtained by insertion of Ag^+ into the preformed cryptand has a simple ^1H NMR spectrum which can only be explained on the basis of high symmetry for the cryptand and cations. The spectrum shows signs of fluxionality at ambient temperatures, but is frozen at 233 K into a pattern which shows just one imino-, one furano- and the expected four methylene signals, demonstrating equivalence for the three strands and the two ends of the cryptand. The ready accommodation of a pair of silver cations within the cryptand held out good prospects of success with the analogous dicopper(I) system.

Results and Discussion

Iminocryptates.—Treatment of L^1 with Cu^I under a nitrogen atmosphere easily generated the dicopper(I) cryptate as a red microcrystalline solid, stable in air as the solid and in solution. Proton NMR spectra are nicely frozen out even at ambient temperatures, making this the least fluxional of the L^1 cryptates we have studied. We have previously noted[7,9,11] the high $\Delta G^‡$ associated with decomplexation of dicopper(I) in other com-
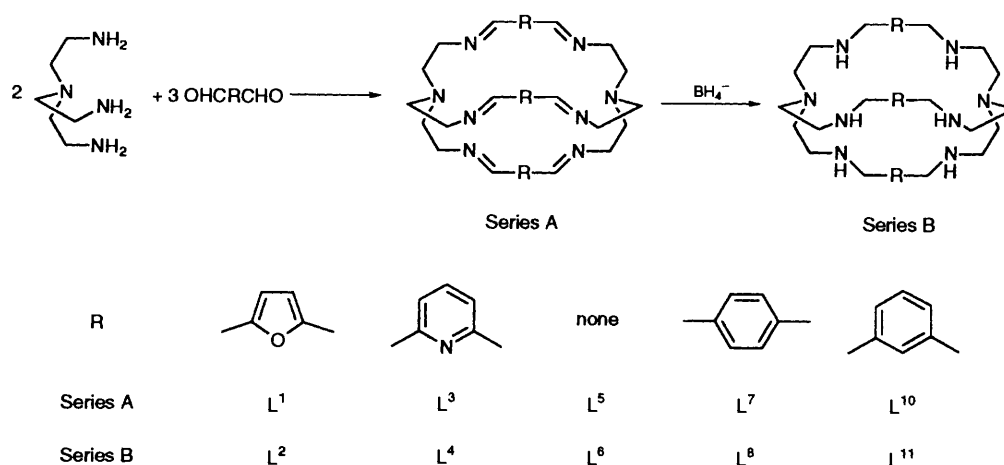
Scheme 1
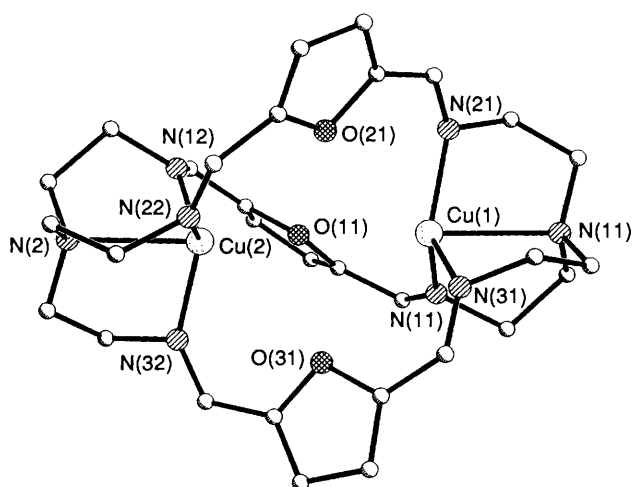
Fig. 1 Perspective view of the cation of complex 1b

(a)   (b)
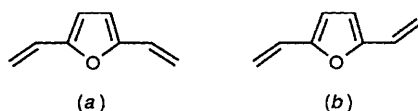
Fig. 2 The *cis,cis* and *trans,trans* conformations of the bis(imino-furan) link

plexes of this iminocryptand series which may contribute to their kinetic stability towards attack by O_2. The simple ^1H NMR spectrum is easily assigned (Table 1) including the well resolved coupling pattern [which involves large ≈ 12–14 Hz geminal H_{ax}–H_{eq} and (13.8 Hz) vicinal H_{ax}–H'_{ax} coupling together with smaller *vic* couplings such as H_{ax}–H'_{eq} of around 3–4 Hz]. There appear to be some slight differences in conformation giving rise to small chemical shift differences in comparison with the disilver cryptate, but the simple pattern which testifies to symmetric placing of the cations within a symmetric host is retained. An X-ray crystallographic structure determination carried out on $[Cu_2L^1][BF_4]_2$ 1b (characterisation data in Table 2) confirms this hypothesis.

Structure of Complex 1b.—Fig. 1 illustrates the structure of complex 1b. Selected bond lengths and angles are given in Table 3. Although the cation has no crystallographic symmetry, there is an approximate three-fold axis running through the copper ions and bridgehead nitrogens. These four atoms are not exactly collinear (Fig. 1). The distance between the bridgehead atoms is now only 8.89 Å, a shortening of 1.5 Å compared with the free macrocycle, which results from adoption of the *cis,cis* [Fig. 2(a)] conformation in the bis(iminofuran) links as against the *trans*,
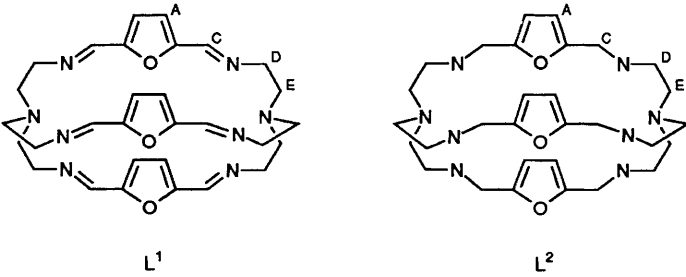
trans [Fig. 2(b)] arrangement adopted in the free macrocycle. Reduction of the N(br) $\cdots$ N(br) distance as against that in the free macrocycle is expected to be a feature of any convergent conformation, and indeed that revealed in the asymmetric monoco-ordinating configuration which exists in $[NaL^1]^+$ is shorter again, at 8.58 Å. (In that case the strong hydrogen bonding of co-ordinated water, held as a second guest within the cavity, may be reponsible for closing up the distance.)

The Cu $\cdots$ Cu distance in complex 1b is 4.2 Å, shorter than that in $[Cu_2L^7]^{2+}$, as expected because of the shorter linker units, but longer than others so far reported for the dicopper(I) iminocryptand series.[6–8] In $[Cu_2L^3]^{2+}$ the copper cations are pulled well out of the N_3 plane by attraction to the hemico-ordinated pyridine,[7] while in $[Cu_2L^5]^{2+}$ the interaction is repulsive and the copper cations are pushed back into the N_3 plane.[6] In the present system the siting of the copper cations relative to the N_3 plane appears to be very nearly tren-determined; it is 0.34 *versus* 0.208 Å out of plane in a four-co-ordinate copper(I) complex of an otherwise similar mono-nucleating trend-derived tri-Schiff base podand.[13] Although it would appear possible to incorporate a single-atom (perhaps even a non-linear two-atom) bridge between copper cations in 1b, any bridging ligand would have to suffer the consequences of close approach to the furan lone pairs. Given the co-ordinative saturation of the copper(I) ion, accommodation of a bridging ligand is unlikely to be an attractive option for the +1 state; however five-co-ordination is common in the +2 state, and possibilities for accommodation of bridges look better there, on the basis of co-ordination geometry, at least.

In an attempt to incorporate single- or two-atom bridges between the copper(I) centres we treated $[Cu_2L^1]^{2+}$ with the neutral ligands pyridazine, CO and O_2. In all three cases, unchanged starting material was recovered. The complex, although thermodynamically capable[14] of being oxidised by O_2, appears kinetically stable against such attack.

Anionic donors are expected to stabilise the +2 state, so it it not surprising that treatment of L^1 with Cu^{II} in undried ethanol generates the dicopper(II) cryptate as a bright green microcrystalline solid $[Cu_2L^1(OH)]^{3+}$ 2. Together with an intense $O^{2-} \rightarrow Cu^{II}$ ligand-to-metal charge-transfer (l.m.c.t.) band at ≈ 400 nm, this product (Table 3) has d–d bands in the solid-state electronic spectrum typical of trigonal-bipyramidal copper(II) co-ordination geometry, something one could normally expect to confirm with the aid of ESR spectroscopy; however, in this case, no spectrum is observable, which suggests the operation of strong antiferromagnetic interaction between the copper(II) paramagnets. We were able to confirm this by measuring the magnetic susceptibility of $[Cu_2L^1(OH)][ClO_4]_3 \cdot 2H_2O$ 2a.

Magnetic susceptibility measurements on Complex 2a. Our first attempts at measuring the magnetic susceptibility using our

Table 1 Proton NMR spectra of L^1, L^2 and derivatives[a]

L^1 L^2

δ

Compound	Solvent	v/MHz	T/K	H_A	H_C	H_D	H_E	Ref.
L^1	CDCl₃	250	293	7.09 (s)	7.73 (s)	3.53 (br s)	2.74 (br s)	
		90	293	7.07 (s)	7.64 (s)	3.76 (d), 3.26 (t)	2.93 (t), 2.56 (d)	10
$[Ag_2L^1][CF_3SO_3]_2$	CD₃CN	500	293	7.17 (s)	8.24 (d)	3.55 (br s), 3.22 (br s)	2.98 (br s), 2.60 (br s)	11
		500	233	7.17 (s)	8.24 (d)	3.54 (t), 3.19 (d)	2.96 (d), 2.55 (t)	
$[Cu_2L^1][ClO_4]_2$	CD₃CN	400	293	7.10 (s)	8.22 (s)	3.42 (m), 3.23 (d)	3.12 (d), 2.67 (t)	This
		400	233	7.10 (s)	8.16 (s)	3.36 (t), 3.15 (d)	3.03 (d), 2.64 (t)	work
L^2	CDCl₃	250	293	6.08 (s)	3.70 (s)		2.57 (s)[b]	This work

[a] All shifts in ppm from SiMe₄: s = singlet, d = doublet, t = triplet, br = broad. [b] H_D, H_E undifferentiated.

Table 2 Analytical, spectroscopic and magnetic data for L^1 and L^2 complexes

Complex	Colour	Analysis (%) C	H	N	Selected IR data (cm⁻¹) v(C=N) or v(NH); v(X)[a]	Electronic spectra[b] λ/nm (ε/dm³ mol⁻¹ cm⁻¹)	μ/μ_B[c] 90	300 K
1a $[Cu_2L^1][ClO_4]_2$· 2H₂O	Red-brown	39.8 (39.2)	4.4 (4.0)	12.2 (12.2)	1629m; 1098m; 621m	410 (4900)	—	—
1b $[Cu_2L^1][BF_4]_2$	Red-brown	41.9 (42.0)	4.0 (4.2)	12.9 (13.1)	1629m; 1049s, 1029s	407 (6800)	—	—
2a $[Cu_2L^1(OH)][ClO_4]_3$· 2H₂O	Bright green	34.9 (34.8)	4.0 (4.0)	10.9 (10.8)	[d]1632m; 1086s, 623m	402 (1900), 720 (319), 880 (290)	0.46	0.82
2b $[Cu_2L^1(OH)][PF_6]_3$· MeCN·H₂O	Bright green	32.3 (32.2)	3.4 (3.3)	10.5 (10.5)	[d]1633m; 873vs, 556ms	404 (1700), 722 (300), 870 (270)	e	e
3 $[Cu_2L^1(im)][ClO_4]_3$	Grey-blue	36.2 (37.8)	3.7 (3.7)	13.3 (14.0)	1680, 1641; 1093vs, 623ms	700 (252)	e	e
4 $[Cu_2L^9(im)][ClO_4]_3$	Deep blue	32.6 (32.5)	4.1 (4.3)	13.5 (14.0)	[f]1638; 1092s, 621m	679 (190)	1.31	1.61
5 $[Cu_2L^2][ClO_4]_2$	White	40.8 (40.3)	5.2 (5.4)	12.6 (12.5)	3274m; 1118s, 1086s, 623m	260 (sh)[g,h]	—	—
6 $[Cu_2L^2(CO)_2][BF_4]_2$	Pale yellow	41.2 (41.5)	5.2 (5.2)	12.5 (12.1)	3294m; 2065m;[i] 1084, 1041, 1027vs	270s (sh),[g,h] 360m (sh)[g]	—	—
7a $[Cu_2L^2(OH)][ClO_4]_3$· MeCN	Emerald green	36.4 (36.5)	5.0 (4.9)	11.9 (12.0)	[d]3271m; 1095s, 623m	360 (4300), 700 (350), 850 (450)	0.61	0.75
7b $[Cu_2L^2(OH)] [CF_3SO_3]_3$	Emerald green	33.8 (33.7)	4.4 (4.4)	9.3 (9.5)	[d]3279m; 1295vs, 1226m, 1067s	358 (4700), 700 (sh), 805 (500)	0.31[j]	0.71
8 $[Cu_2L^2(im)][ClO_4]_3$· H₂O	Blue	36.4 (36.7)	4.5 (4.9)	13.0 (13.0)	3297m; 1095vs, 623m	349 (2300), 671 (570), 700 (540)	1.37	1.77
9 $[Cu_2L^2(N_3)][CF_3SO_3]_3$	Golden brown	33.6 (33.6)	3.8 (3.6)	12.7 (13.0)	3232m, 2185s,[k] 1254vs 1167s, 1139s, 1031vs	460,[g] 660,[g] 900[g]	1.91[l]	1.93

[a] X = ClO₄, CF₃SO₃, BF₄ or PF₆. [b] In 10^{-3} mol dm⁻³ MeCN, c.t. or d–d. [c] Moment per Cu²⁺ ion. [d] v(OH) 3550–3560 cm⁻¹. [e] Not investigated. [f] v(NH₂) at 3326 and 3267 cm⁻¹. [g] Nujol mull. [h] π–π* transition. [i] v(CO). [j] Value at 6 K: 0.21 μ_B. [k] v(N₃⁻). [l] Value at 49 K: 2.03 μ_B.

resistive Faraday susceptibility system confirmed the essential diamagnetism of the complex over the temperature range 4–300 K. As this equipment lacked the necessary sensitivity to make very accurate measurements with such a low-susceptibility compound, more accurate measurements (see SUP 56998) were carried out using a SQUID susceptometer at Grenoble. The molar susceptibility per copper ion (Fig. 3) was fitted to the Bleaney–Bowers equation (1) based on the Hamiltonian

$$\chi_m = (Ng^2\beta^2/3kT)[1 + \tfrac{1}{3}\exp(-2J/kT)]^{-1}(1 - P) + PNg^2\beta^2/4kT + \text{t.i.p.} \quad (1)$$

$-2JS_1 \cdot S_2$ for two interaction spins $\tfrac{1}{2}$, modified to take into account temperature-independent paramagnetism (t.i.p) and the contribution of a small percentage (P) of monomeric

paramagnetic impurity. The best fit was obtained using a $-2J$ value of 965 cm⁻¹, $g = 2.05$ and t.i.p. = 1×10^{-4} cm³ mol⁻¹.

Such a large antiferromagnetism, at the upper limit[15] of those known for a pair of copper(II) ions separated by a single hydroxo bridge, implies efficient mediation of magnetic exchange. Lack of long-term solution stability prevented growth of crystals of sufficient size to confirm our suspicion that the efficient antiferromagnetic exchange derives from enforced linearity of the Cu–O–Cu nuclei; on standing, the solution changes from bright green to blue green, indicative of the implied change of co-ordination geometry consequent upon ring opening. Such hydrolytic attack is common in the hexamino series; indeed, a pure sample of the dicopper(II) complex $[Cu_2L^9(im)][ClO_4]_3$ **4** was obtained in attempts to purify the crude $[Cu_2L^1(im)][ClO_4]_3$ product **3** (Him =

L⁹
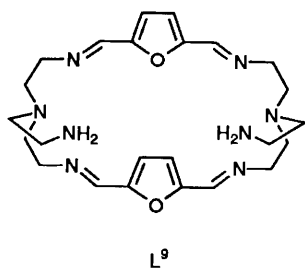
Table 3 Selected bond lengths (Å) and angles (°) for complex **1b**

Cu(1)–N(1)	2.388(4)	Cu(1)–N(11)	1.991(4)
Cu(1)–N(21)	1.981(4)	Cu(1)–N(31)	2.024(4)
Cu(2)–N(2)	2.397(4)	Cu(2)–N(12)	2.003(4)
Cu(2)–N(22)	1.986(4)	Cu(2)–N(32)	2.006(4)
N(1)–Cu(1)–N(11)	81.7(1)	N(1)–Cu(1)–N(21)	79.7(1)
N(11)–Cu(1)–N(21)	123.5(2)	N(1)–Cu(1)–N(31)	79.0(1)
N(11)–Cu(1)–N(31)	111.3(1)	N(21)–Cu(1)–N(31)	116.5(1)
N(2)–Cu(2)–N(12)	79.3(1)	N(2)–Cu(2)–N(22)	80.8(1)
N(12)–Cu(2)–N(22)	119.2(1)	N(2)–Cu(2)–N(32)	80.1(1)
N(12)–Cu(2)–N(32)	112.3(2)	N(22)–Cu(2)–N(32)	119.8(2)
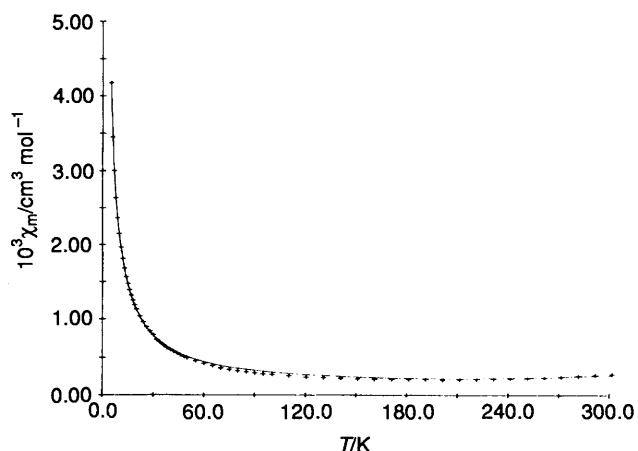
Fig. 3 Variation of magnetic susceptibility per Cu ion with temperature for [Cu₂L¹(OH)][ClO₄]₃·2H₂O **2a**. (●) experiment, —— theory [see equation (1)]

imidazole) by recrystallisation. Apart from the low-quality sample of **3**, no other bridged complexes of L¹ were obtained, which is unsurprising given the steric constraints existing in this relatively rigid ligand.

A similar μ-OH derivative of the related ligand L¹⁰ has been isolated and will be described elsewhere.[16] The copper(II) chemistry of L¹⁰ is in general similar to that of L⁷, but two differences are noticeable.[9,5,16] The hydroxo-bridged derivative of L⁷ shows superior solution stability to that of the L¹⁰ analogue. Moreover, L¹⁰ forms an azido-bridged derivative, which is absent in the L¹ system. The enforced proximity of the furan lone pair may be responsible both for stabilisation of the hydroxo-bridge (because of hydrogen bonding) and destabilisation of the azido-bridge (because of repulsive interaction with the azide π system).

In order to avoid hydrolytic ring opening and to extend the range of bridging links that could be studied, we investigated the host properties of the octaamine cryptand, L², derived from L¹ by tetrahydroborate reduction.

Aminocryptates.—(*i*) *The dicopper(*I*) system.* This 'harder' all-sp³ N ligand, L², can be expected to stabilise copper(II) in

relation to copper(I). Thus, although treatment with copper(I) salts under anaerobic conditions generates the dicopper(I) cryptate [Cu₂L²][ClO₄]₂ **5** as a microcrystalline white solid, it quickly acquires a greenish tinge even in the solid state. In solution it oxidises rapidly to copper(II), preventing acquisition of NMR spectra, for example. Thus it seems that the kinetic stabilisation against attack by oxygen which characterises[14] the hexaimine cryptates (and at least one[4] of the octaamine derivatives we have studied) is not operating here.

The compound is also more susceptible to attack by carbon monoxide. On bubbling CO through an MeCN–MeOH solution a white precipitate was formed which showed an infrared absorption at 2065 cm⁻¹, suggestive of terminally bonded CO. This product showed slightly greater redox stability than the parent dicopper(I) complex, retaining its pale yellow colour in solution for around an hour in air while **5** acquired a green colour within seconds; similarly the solid product [Cu₂L²(CO)₂][BF₄]₂ **6** can be stored in air for months while **5** turns green within days.

(*ii*) *Dicopper(*II*) complexes.* Treatment of L² with copper(II) salts in the presence of base gave μ-hydroxo-dicopper(II) complexes [Cu₂L²(OH)]³⁺ **7** in good yield as bright green needles. The solid-state electronic spectrum is similar to that of **2** in respect of splitting of d–d bands and position of the l.m.c.t. absorption, suggesting once more a trigonal-bipyramidal co-ordination geometry around copper(II). Other similarities include the very sharp ν(OH) infrared absorption close to 3550 cm⁻¹ and the very small magnetic susceptibility. An X-ray crystallographic structure determination of [Cu₂L²(OH)]-[CF₃SO₃]₃ **7b** has been reported in preliminary communication[17] and is described in full in this paper.

In line with the greater flexibility anticipated for this octaamine host, bridges other than single-atom μ-OH⁻ could be accommodated between the copper(II) cations held within L². Thus treatment with a stoichiometric amount of imidazole and azide generated the blue μ-imidazolate complex [Cu₂L²(im)][ClO₄]₃·H₂O **8** and the golden-brown μ-azido complex [Cu₂L²(N₃)][CF₃SO₃]₃ **9** respectively. The different colours of these complexes derive partly from l.m.c.t. absorptions, although **8** does show a d–d spectrum different from the rest, suggesting either square-pyramidal or tetragonal geometry, the latter necessarily requiring solvent co-ordination. In addition to the pair of medium-weak absorptions near 11 600 and 14 400 cm⁻¹, which typify trigonal-bipyramidal co-ordination geometry, complex **9** shows a broad and intense N₃⁻→Cuᴵᴵ l.m.c.t. absorption at 460 nm which tails into the visible. As well as this unusually low-frequency band, it shows an exceptionally high νₐₛᵧₘ(N₃⁻) infrared absorption, at 2185 cm⁻¹. These are properties which have been[5] associated with the existence of a linear Cu–NNN–Cu entity.

Complex **7b.** Fig. 4 illustrates siting and geometry of the Cu–O(H)–Cu entity within the cryptand. It will be immediately noticed that the link is virtually linear (Cu–O–Cu 174°) and that the copper(II) site is effectively trigonal bipyramidal. The copper atoms are slightly out of the equatorial triimino-N plane (0.222 and 0.227 Å) in the direction of the hydroxo-bridge and the axial ligands (N_br and OH⁻) are at closer distances than the equatorial N(H) donors (Table 4). The molecule lacks any crystallographically imposed symmetry, and a moderately strong (2.819 Å) OH···O(furan) hydrogen bond connects O(1) and O(11). Although the other O(H)···O(furan) distances are not more than 0.1 Å longer than this distance, there is no sign of any disorder to indicate a fluxional, rotating hydrogen bond in the solid state, so the other two relatively short O···O contacts may result from steric necessity. The slight deviation from linearity in the Cu–O(H)–Cu angle derives from displacement of OH towards the furan oxygen with which it is hydrogen bonded. The Cu···Cu distance is 3.90 Å and the axial length N_br···N_br of the cryptand is 8.05 Å, *i.e.* shorter even than in the monosodium cryptate.[12] The disposition of the furan rings which respect to the dicopper site is unusual; for the

Table 4 Selected bond lengths (Å) and angles (°) for complex **7b**

Cu(1)–O(1)	1.957(4)	Cu(1)–N(1)	2.075(5)
Cu(1)–N(31)	2.129(5)	Cu(1)–N(21)	2.144(5)
Cu(1)–N(11)	2.173(5)	Cu(2)–O(1)	1.948(4)
Cu(2)–N(2)	2.074(5)	Cu(2)–N(32)	2.130(5)
Cu(2)–N(22)	2.149(5)	Cu(2)–N(12)	2.182(6)
O(1)–Cu(1)–N(1)	178.0(2)	O(1)–Cu(1)–N(31)	97.0(2)
N(1)–Cu(1)–N(31)	83.7(2)	O(1)–Cu(1)–N(21)	96.8(2)
N(1)–Cu(1)–N(21)	84.3(2)	N(31)–Cu(1)–N(21)	124.9(2)
O(1)–Cu(1)–N(11)	93.8(2)	N(1)–Cu(1)–N(11)	84.2(2)
N(31)–Cu(1)–N(11)	116.9(2)	N(21)–Cu(1)–N(11)	114.9(2)
O(1)–Cu(2)–N(2)	178.8(2)	O(1)–Cu(2)–N(32)	96.7(2)
N(2)–Cu(2)–N(32)	84.4(2)	O(1)–Cu(2)–N(22)	96.2(2)
N(2)–Cu(2)–N(22)	83.2(2)	N(32)–Cu(2)–N(22)	119.0(2)
O(1)–Cu(2)–N(12)	95.2(2)	N(2)–Cu(2)–N(12)	84.2(2)
N(32)–Cu(2)–N(12)	121.9(2)	N(22)–Cu(2)–N(12)	115.8(2)
Cu(2)–O(1)–Cu(1)	174.0(3)		

first time [Fig. 4(*b*)] a structure shows the aromatic spacer units triangularly rather than trigonally disposed about the bridgehead axis, close to the conformation found in most of the free iminocryptands where the donor line pairs are divergently arranged. In the present structure, because of the flexibility about sp³ N, the convergent-donor conformation can be associated with a good degree of steric protection offered by the furan rings.

Dicopper(ii) *Complexes: Magnetic and ESR Measurements.*— The bridged dicopper(ii) complexes **2** and **7–9** illustrate almost the complete range of magnetic behaviour (SUP 56998) available to a pair of interacting copper(ii) ions. As we have already described, **2a** is virtually diamagnetic, with a $-2J$ value approaching $1000\ cm^{-1}$; **7b** exhibits barely less efficient ($-2J =$ $865\ cm^{-1}$) antiferromagnetic interaction (Table 5).

The magnetic 'silence' of these compounds was confirmed by ESR measurements in both glass and solid states. On the basis of the similarity of the magnetic and spectroscopic behaviour of these two μ-hydroxo-dicopper cryptates, the established near-linearity[17] of the N_{br}–Cu–O(H)–Cu–N_{br} link in **7** can be extrapolated to **2**. Such linearity allows the most advantageous overlap between the d_{z^2} magnetic orbitals in trigonal-bipyramidal copper(ii) and O $2p_z$ of the bridging hydroxide, rationalising the efficient antiferromagnetic exchange.

For the μ-imidazolate complex **8**, moderate antiferromagnetic interaction was mediated *via* the heterocyclic bridge, leading to observation of a broad maximum (Fig. 5) in the plot of magnetic susceptibility *versus* temperature, at around 80–100 K, and an estimate of the magnetic exchange coupling constant, $-2J$, of about $92\ cm^{-1}$. This is of the same order as those evaluated from some other μ-imidazolate cryptates[5,16] but slightly greater than for less sterically constraining macrocyclic or acyclic imidazolate-bridged dimers.[18,19] The most important geometric parameter governing interaction in bridged dicopper imidazolate complexes is believed to be the Cu–N–N angle;[20] the largest interactions so far recorded are associated with large values of this angle, which permits the most efficient σ-superexchange route.

As expected, the ESR spectrum of complex **8** shows significant zero-field splitting ($D \approx 900$ G) and a relatively intense ($\approx 1/10$th intensity of the $g \approx 2$ signal) hyperfine-split ($A = 60$ G) half-band, both ESR signatures of copper(ii) dimers bridged by unsaturated azaheterocycles.[19] The ESR observation suggests the operation, under ESR conditions, of an excited-state π-superexchange pathway,[21] *e.g.* $d_{yz} \longrightarrow \pi^*$.

The μ-azido complex **9**, the electronic and vibrational spectra of which suggest a linearly bridged 1,3-azido mode, exhibits magnetic behaviour similar to that reported[5] for other μ-azido complexes believed to contain the linear Cu–NNN–Cu entity. The χ *vs.* T plot corresponds to a magnetic moment which

Table 5 Magnetic properties of dicopper(ii) complexes

Complex	$-2J/$ cm^{-1}	g	$10^6 t.i.p./$ $cm^3\ mol^{-1}$	Impurity (%)
2a $[Cu_2L^1(OH)][ClO_4]_3\cdot$ $2H_2O$	965 ± 50	2.05	100	2.6
4 $[Cu_2L^9(im)][ClO_4]_3$	89 ± 10	2.022	0	0
7b $[Cu_2L^2(OH)][CF_3SO_3]_3$	865 ± 50	2.13	90	1.2
8 $[Cu_2L^2(im)][ClO_4]_3\cdot$ H_2O	92 ± 10	2.05	180	3.5
9 $[Cu_2L^2(N_3)][CF_3SO_3]_3$	−4 ± 2	2.13	190	

(*a*)

(*b*)
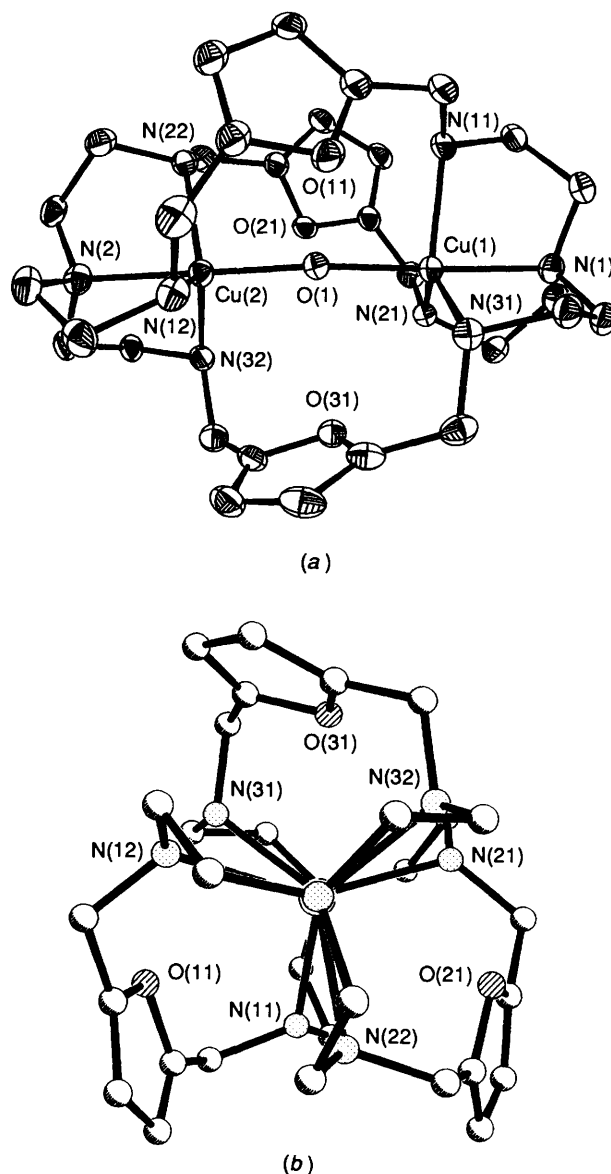
Fig. 4 Perpsective view of the ciation of complex **7b**; (*a*) at right angles to the $N_{br} \cdots N_{br}$ axis, (*b*) along the $N_{br} \cdots N_{br}$ axis

increases slightly with decrease in temperature, fitting a magnetic exchange coupling constant $-2J$ of $+4\ cm^{-1}$, *i.e.* a weak ferromagnetic interaction. The ESR spectrum likewise suggests a triplet ground state because the one conclusion that can confidently be drawn from this unusual spectrum (Fig. 6) is that the zero-field splitting is very large. The spectrum spreads over ≈ 5 kG and includes a $g = 7$ feature of comparable intensity to that of the $g \approx 2$ signal. Such an intense low-field feature appears to be characteristic of linear 1,3-azido-bridged
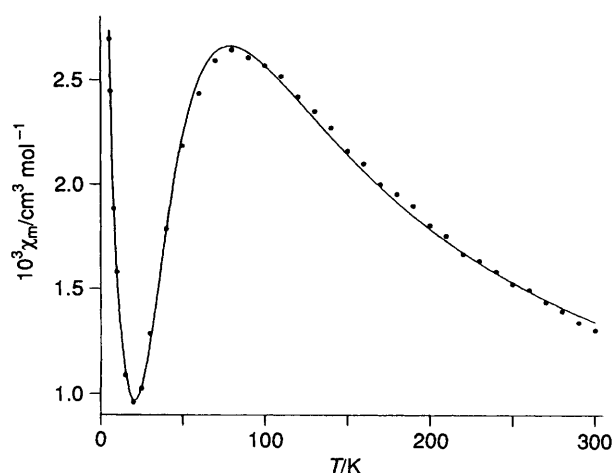
Fig. 5 Variation of magnetic susceptibility per Cu ion with temperature for $[Cu_2L^2(im)][ClO_4]_3 \cdot H_2O$ 8. (●) Experiment, ———, theory [see equation (2)]

dicopper cryptates, and we are currently attempting to simulate the spectra using large zero-field parameters.

Electrochemistry.—Cyclic voltammetry of complex 1 showed irreversible behaviour;[14] an oxidation wave at 280 mV *vs.* ferrocene–ferrocenium has no reduction component, but is accompanied by an irreversible reduction close to -500 mV with a scan rate-dependent potential which suggests a coupled chemical reaction of the electrochemical-chemical-electrochemical type. The octaamine dicopper(I) cryptate 5 displays a similar pattern, but both waves are shifted by over 350 mV to negative potential ($E_a = -97$, $E_c' = -875$ mV), reflecting the anticipated stabilisation of the higher oxidation state of copper co-ordinated within this harder sp^3 N host. One candidate for the process giving rise to the irreversible electrochemistry of both dicopper(I) cryptates is solvent co-ordination in the higher oxidation state; another is the incorporation of a μ-hydroxo bridge.

The presence of the μ-azido link in complex 9 affects the electrochemistry. As well as stabilising the $+2$ state, which shifts redox potentials to more negative values, the system now shows some reversibility. A pair of quasi-reversible overlapped waves centred around -870 and -700 mV is seen, suggesting, as with the analogous L^4 complex, that two sequential one-electron redox processes are in operation, following the scheme $Cu^{II}-Cu^{II} \longrightarrow Cu^{II}-Cu^{I} \longrightarrow Cu^{I}-Cu^{I}$, which involves a mixed-valence species.

Conclusion

The azacryptand hosts investigated generate dicopper cryptates which excemplify a wide range of magnetic behaviour and redox state preferences. The hexaimine cryptand L^1 can accommodate a pair of copper(I) cations with 4.2 Å separation, or a μ-hydroxo-dicopper(II) assembly, but no other dicopper(II) complexes of this ligand were characterised. With the octaamine cryptand L^2, on the other hand, air-sensitive copper(I) complexes are obtained, but a wide range of stable dicopper(II) complexes are also found. Bridging links studied include the single atom hydroxide and the bent three-atom imidazolate as well as the linear three-atom azido. Magnetic interactions range from weak ferromagnetism in the μ-azido L^2 complex to virtual magnetic 'silence' in the μ-hydroxo complexes of both ligands. The origin of the strong antiferromagnetic interaction in a collinear disposition of copper d$_{z^2}$ and oxygen 2p$_z$ orbitals has been confirmed by X-ray crystallography.
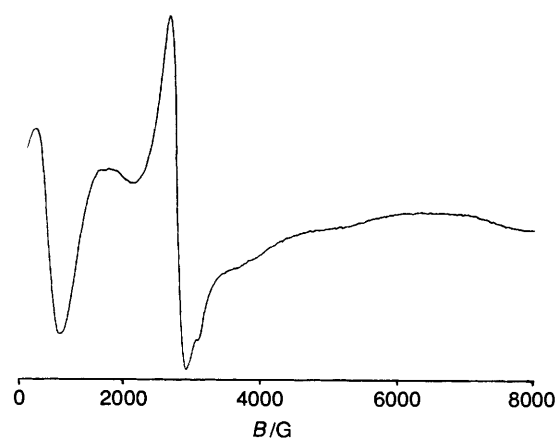

Fig. 6 The X-band ESR spectrum of $[Cu_2L^2(N_3)][CF_3SO_3]_3$ 9 as a polycrystalline solid at -160 °C

Experimental

Preparations.—L^1. To a methanolic solution of tren (2 mmol, 0.3 cm^3) was added dropwise a solution of 2,5-diformylfuran (3 mmol, 0.37 g) in MeOH (50 cm^3). The solution was refluxed for 3 h during which it became bright yellow. After cooling, the volume was reduced to 20 cm^3 and an equal volume of MeCN added. After a day or two of slow evaporation the cryptand was obtained as transparent cubes in 62% yield.

$[Cu_2L^1]X_2 \cdot yH_2O$ (X = ClO_4^-, $y = 2$ **1a**; X = BF_4^-, $y = 0$ **1b**). The compound L^1 (2 mmol, 0.11 g) was dissolved in deoxygenated methylene chloride (30 cm^3) and a solution of $[Cu(MeCN)_4]X$ in deoxygenated MeCN (30 cm^3) was added. After 15 min, deoxygenated EtOH was added and the volume reduced to 20 cm^3). The red microcrystalline product was obtained in 60–80% yield.

$[Cu_2L^1(OH)]X_3$ (X = ClO_4 **2a** *or* PF$_6$ **2b**). Compound L^1 (0.05 mmol, 0.3 g) was dissolved in methylene chloride (30 cm^3) and the copper(I) salt (1.1 mmol, 0.4 g) in EtOH–MeCN (1 : 1, 50 cm^3) added. After reducing the volume rapidly on a rotary evaporator, tiny green crystals of product were obtained in 73% yield.

$[Cu_2L^1(im)][ClO_4]_3$ 3 *and* $[Cu_2L^9(im)][ClO_4]_3$ 4. To L^1 (0.5 mmol, 0.3 g) in methylene chloride (30 cm^3) were added imidazole (0.06 mmol, 0.04 g) EtOH (10 cm^3) and $Cu(ClO_4)_2 \cdot 6H_2O$ (1.1 mmol) in EtOH (30 cm^3). A grey-blue solid was isolated in 77% yield. Recrystallisation of this solid from MeCN–EtOH gave dark blue crystals of complex 4. Although satisfactory C,H,N analysis could not be obtained for 3, the FAB mass spectrum confirmed the presence of L^1, together with a partly hydrolysed ligand (L^1 + H$_2$O). The FAB mass spectrum unambiguously confirmed (base peak at $m/z = 531$ corresponding to $[CuL^9]^+$) the presence of the dipendant amine macrocycle L^9 in 4 as well as the absence of cryptand L^1.

L^2. The octaamine was prepared by *in situ* reduction of L^1. 2,5-Diformylfuran (6 mmol, 7.5 g) was dissolved in MeOH (200 cm^3) and stirred for 1 h at room temperature with a solution of tren (4 mmol in 50 cm^3). Then an excess of NaBH$_4$ (≈ 100 mmol) was added in small portions and the reaction mixture stirred at room temperature for 72 h. The mixture was worked up in the normal way by CHCl$_3$ extraction from strong NaOH aqueous solution and the reduced macrocycle was obtained in 68% yield.

$[Cu_2L^2][ClO_4]_2$ 5. To L^2 (0.5 mmol, 0.3 g) dissolved in deoxygenated EtOH (50 cm^3) was added $[Cu(MeCN)_4]ClO_4$ (1.05 mmol, 0.34 g) in MeCN (30 cm^3). The reaction mixture was heated to 50 °C under a stream of N$_2$ or Ar until solid appeared. It was then cooled in ice and filtered under N$_2$. Yield 72%.

$[Cu_2L^2(CO)_2][BF_4]_2$ 6. A solution of L^2 (0.25 mmol, 0.15 g) dissolved in deoxygenated MeOH (50 cm^3) was saturated with CO at room temperature, and $[Cu(MeCN)_4]BF_4$ (0.52 mmol, 0.17 g) in deoxygenated MeCN (30 cm^3) was added. Carbon

Table 6 Atomic coordinates ($\times 10^4$)

Atom	x	y	z	Atom	x	y	z
Complex 1b							
Cu(1)	6 959(1)	9 845(1)	2 240(1)	N(22)	9 280(3)	10 845(2)	−56(3)
Cu(2)	8 360(1)	11 294(1)	832(1)	C(28)	10 272(4)	11 231(2)	−212(4)
N(1)	6 290(3)	8 990(2)	3 051(3)	C(29)	9 812(4)	11 816(2)	−691(3)
N(2)	9 082(3)	12 118(2)	−39(3)	C(30)	7 271(4)	8 579(2)	3 177(3)
C(10)	5 981(4)	9 249(2)	3 976(3)	C(31)	8 076(4)	8 709(2)	2 397(3)
C(11)	6 745(4)	9 785(2)	4 299(3)	N(32)	8 404(3)	9 348(2)	2 468(3)
N(11)	6 631(3)	10 241(2)	3 494(3)	C(32)	9 373(4)	9 458(2)	2 985(3)
C(12)	6 220(4)	10 741(2)	3 720(3)	C(33)	9 834(4)	10 040(2)	3 220(3)
C(13)	5 943(4)	11 235(2)	3 048(3)	C(34)	10 716(4)	10 191(2)	3 909(3)
C(14)	5 256(4)	11 712(2)	3 161(4)	C(35)	10 807(4)	10 821(2)	3 886(3)
C(15)	5 171(4)	12 032(2)	2 257(4)	C(36)	9 985(4)	11 013(2)	3 165(3)
C(16)	5 829(4)	11 746(2)	1 651(4)	O(31)	9 362(3)	10 543(1)	2 739(2)
O(11)	6 312(3)	11 243(1)	2 121(2)	C(37)	9 786(4)	11 610(2)	2 799(3)
C(17)	6 082(4)	11 911(2)	671(3)	N(32)	9 152(3)	11 757(2)	1 991(3)
N(12)	6 895(3)	11 681(2)	244(3)	C(38)	9 150(5)	12 397(2)	1 720(3)
C(18)	7 068(4)	11 952(2)	−725(3)	C(39)	9 693(4)	12 476(2)	761(3)
C(19)	8 045(4)	12 402(2)	−559(3)	B(1)	7 530(5)	3 833(3)	1 378(5)
C(20)	5 314(4)	8 782(2)	2 358(3)	F(11)	6 797(3)	3 357(1)	1 187(3)
C(21)	4 823(4)	9 303(2)	1 709(3)	F(12)	8 250(3)	8 864(1)	637(2)
N(21)	5 753(3)	9 560(2)	1 191(3)	F(13)	6 921(3)	4 361(1)	1 385(2)
C(22)	5 758(4)	9 407(2)	275(3)	F(14)	8 200(3)	3 762(2)	2 283(2)
C(23)	6 607(4)	9 566(2)	−347(3)	B(2)	3 013(6)	2 471(3)	4 651(5)
C(24)	6 781(4)	9 346(2)	−1 250(3)	F(21)	2 756(3)	2 979(2)	5 125(3)
C(25)	7 767(4)	9 627(2)	−1 512(3)	F(22)	2 064(3)	2 114(2)	4 505(3)
C(26)	8 128(4)	10 014(2)	−766(3)	F(23)	3 336(4)	2 622(2)	3 726(3)
O(21)	7 431(3)	9 985(1)	−26(2)	F(24)	3 906(3)	2 163(1)	5 172(2)
C(27)	9 078(4)	10 424(2)	−690(3)	O(1)	2 125(8)	1 858(4)	2 125(6)
Complex 7b							
Cu(1)	3 987(1)	8 322(1)	1 692(1)	C(33)	1 403(5)	8 987(4)	2 149(3)
Cu(2)	3 805(1)	8 282(1)	3 434(1)	C(34)	630(6)	8 902(4)	2 550(4)
O(1)	3 918(4)	8 244(3)	2 565(2)	C(35)	1 000(6)	9 297(4)	3 084(3)
N(1)	4 094(4)	8 368(3)	766(2)	C(36)	1 985(5)	9 595(4)	2 987(3)
N(2)	3 686(5)	8 299(3)	4 359(2)	O(31)	2 239(3)	9 422(2)	2 401(2)
C(10)	4 759(5)	7 683(4)	569(3)	C(37)	2 786(5)	10 018(4)	3 361(3)
C(11)	5 637(5)	7 495(4)	1 050(3)	N(32)	3 781(4)	9 537(3)	3 512(2)
N(11)	5 122(4)	7 351(3)	1 630(2)	C(38)	4 162(5)	9 676(4)	4 149(3)
C(12)	4 748(7)	6 520(4)	1 691(3)	C(39)	3 513(6)	9 142(4)	4 543(3)
C(13)	4 396(6)	6 328(4)	2 302(3)	S(41)	7 744(2)	9 382(1)	208(1)
C(14)	4 854(6)	5 909(4)	2 768(3)	O(41)	7 333(5)	8 656(4)	412(3)
C(15)	4 129(6)	5 955(4)	3 243(3)	O(42)	7 102(5)	10 048(3)	435(3)
C(16)	3 284(6)	6 392(4)	3 058(3)	O(43)	8 008(4)	9 477(4)	−405(2)
O(11)	3 410(4)	6 624(3)	2 463(2)	C(41)	9 025(10)	9 515(9)	615(4)
C(17)	2 328(6)	6 705(4)	3 358(3)	F(41)	9 631(5)	8 868(5)	412(3)
N(12)	2 336(4)	7 579(3)	3 450(2)	F(42)	9 442(5)	10 222(5)	530(3)
C(18)	1 880(6)	7 810(4)	4 032(3)	F(43)	8 853(5)	9 471(6)	1 214(2)
C(19)	2 768(6)	7 786(4)	4 518(3)	S(51)	−10(2)	6 517(1)	2 124(1)
C(20)	4 601(5)	9 139(4)	609(3)	O(51)	727(5)	6 821(4)	1 712(4)
C(21)	4 315(5)	9 767(4)	1 063(3)	O(52)	−336(5)	7 058(4)	2 586(3)
N(21)	4 691(4)	9 478(3)	1 669(2)	O(53)	237(4)	5 731(3)	2 325(2)
C(22)	5 881(5)	9 631(4)	1 770(3)	C(51)	−1 231(8)	6 394(6)	1 656(4)
C(23)	6 412(5)	9 042(4)	2 167(3)	F(51)	−2 044(4)	6 157(4)	1 985(3)
C(24)	7 215(6)	8 523(4)	2 089(3)	F(52)	−1 118(4)	5 839(4)	1 235(2)
C(25)	7 337(6)	8 068(5)	2 626(3)	F(53)	−1 532(5)	7 065(4)	1 390(3)
C(26)	6 590(6)	8 341(4)	3 004(3)	S(61)	7 042(1)	4 070(1)	166(1)
O(21)	6 017(3)	8 957(3)	2 735(2)	O(61)	6 781(5)	3 306(3)	415(2)
C(27)	6 305(6)	8 117(5)	3 620(3)	O(62)	6 592(4)	4 215(3)	−435(2)
N(22)	5 277(5)	7 660(3)	3 645(2)	O(63)	8 145(3)	4 313(3)	267(2)
C(28)	5 158(7)	7 341(4)	4 259(3)	C(61)	6 296(6)	4 753(5)	627(3)
C(29)	4 708(6)	6 992(4)	4 649(3)	F(61)	5 250(4)	4 605(4)	605(2)
C(30)	2 983(5)	8 308(4)	481(3)	F(62)	6 445(4)	5 502(3)	465(2)
C(31)	2 328(5)	7 755(4)	856(3)	F(63)	6 633(4)	4 687(3)	1 213(2)
N(31)	2 339(4)	8 063(3)	1 485(2)	O(71)	5 752(6)	2 045(5)	1 126(3)
C(32)	1 526(5)	8 701(4)	1 531(3)	O(81)	7 776(8)	1 269(6)	1 323(5)

monoxide was bubbled through the solution until a pale yellow precipitate was obtained in 31% yield.

$[Cu_2L^2(OH)]X_3$ (X = ClO_4, **7a** *or* CF_3SO_3 **7b**). To L^2 (1/6 mmol) dissolved in EtOH (20 cm³) and MeCN (5 cm³) was added the CuX_2 salt (1/3 mmol) in EtOH (10 cm³) in the presence of pyrazole (1/8 mmol) as base. The deep green solution was reduced slowly in air and green needles of product were obtained in 50–60% yield.

$[Cu_2L^2(im)][ClO_4]_3$ **8**. The compound L^2 (0.5 mmol, 0.3 g) was dissolved in MeCN–EtOH (1:1, 30 cm³) and imidazole

(0.5, 0.035 g) was added, followed by $Cu(ClO_4)_2 \cdot 6H_2O$ (1 mmol, 0.35 g) in EtOH (20 cm^3), and the volume was allowed to reduce slowly in air to yield blue crystals in 63% yield.

$[Cu_2L^2(N_3)][CF_3SO_3]_3$ 9. To L^2 (0.5 mmol, 0.3 g) in MeCN–EtOH (1 : 1, 30 cm^3) was added $Cu(CF_3SO_3)_2$ (1 mmol, 0.38 g) in EtOH (20 cm^3) and NaN_3 (0.04 mmol, 0.33 g) in water (1/2 drop). The mixture was left to stand in air and golden crystals of product was filtered off in 59% yield. This product showed (on comparison of mull and solution electronic spectra) a tendency to rearrange in solution.

Physical measurements were made as described in earlier publications.[5,7,14]

X-Ray Crystallography.—Complex **1b**. *Crystal data.* $C_{30}H_{36}$-$B_2Cu_2F_8N_{11}O_{3.5}$, red block, crystal dimensions 0.52 × 0.22 × 0.20 mm, monoclinic, space group $P2_1/c$, $a = 11.776(3)$, $b = 22.375(6)$, $c = 13.449(4)$ Å, $\beta = 97.20(2)°$, $U = 3529(2)$ Å^3, $\mu = 1.29$ mm^{-1}, $Z = 4$, $D_c = 1.629$ g cm^{-3}, $F(000) = 1760$.

Data were collected at 198 K on a Nicolet R3m four-circle diffractometer using graphite-monochromated Mo-Kα radiation ($\lambda = 0.710\,73$ Å). The unit-cell parameters were determined by least-squares refinement of 25 accurately centred reflections ($4 < 2\theta < 33°$). Using 1.6° ω scans at 4.88° min^{-1}, 4871 reflections were collected in the range $4 < 2\theta < 45°$. Of these, 4610 were unique and the 3280 having $F > 6\sigma(F)$ were used in the refinement. Crystal stability was monitored by recording three check reflections every 97 and no significant variations were observed. The data were corrected for Lorentz and polarisation effects and an empirical absorption correction was applied, based on ψ-scan data ($T_{min} = 0.74$, $T_{max} = 0.87$).

The structure was solved by direct methods, which revealed the positions of all the non-hydrogen atoms. It was refined by full-matrix least-squares techniques. All the non-hydrogen atoms were assigned anisotropic thermal parameters. Hydrogen atoms were inserted at calculated position, using a riding model with a common, fixed isotropic thermal parameter. The refinement, in 482 parameters, converged with $R = 0.035$ and $R' = 0.043$. The function minimixed in the refinement was $\Sigma w(F_o - F_c)^2$ where $w = [\sigma^2(F_o) + 0.0006F_o^2]^{-1}$. The final difference map showed no residual electron density greater than ±0.5 e Å^{-3}. All programs used in data reduction, structure solution and refinement are contained in the SHELXTL-PC package.[22] Final atomic coordinates are given in Table 6.

Complex **7b**. *Crystal data.* $C_{33}H_{51}Cu_2F_9N_8O_{14}S_3$, green block, crystal dimensions 0.56 × 0.42 × 0.30 mm, monoclinic, space group $P2_1/n$, $a = 12.434(3)$, $b = 16.919(4)$, $c = 22.300(4)$ Å, $\mu = 1.147$ mm^{-1}, $Z = 4$, $D_c = 1.669$ g cm^{-3}, $F(000) = 2416$.

Data were collected at 143 K on a Siemens P4 four-circle diffractometer using graphite-monochromated Mo-Kα radiation ($\lambda = 0.710\,13$ Å). Unit-cell parameters were determined by non-linear least-squares refinement of 27 accurately centred reflections ($18 < 2\theta < 25°$). Using 2° ω scans at 5° min^{-1}, 7273 reflections were collected in the range $4 < 2\theta < 47°$, 6914 unique reflections ($R_{int} = 0.017$) being used in the refinement. Crystal stability was monitored by recording three check reflections every 97 and the data were scaled to allow for an observed drop of 6% in intensity. The data were corrected for Lorentz and polarisation effects and an empirical absorption correction was applied based on ψ-scan data ($T_{max} = 0.791$, $T_{min} = 0.721$).

The structure was solved by direct methods,[23] which revealed most of the non-hydrogen atoms, and the remaining atoms were located from Fourier difference maps. The solvate water molecule was disordered and this was modelled with 50% occupancy of each of two sites. All the non-hydrogen atoms, other than in the disordered water molecule, were assigned anisotropic thermal parameters. Hydrogen atoms were inserted at calculated positions with a common, fixed isotropic thermal

parameter except for those on the water solvate molecule and the central hydroxo bridge, which were not included. All the data were used for refinement on F^2 which converged with $wR2 = 0.168$ (all data), goodness of fit $= 1.065$ and the conventional $R1 = 0.0596$ $[I > 2\sigma(I)]$ for 611 parameters. The function minimised in the refinement was $wR2 = \{\Sigma[w(F_o^2 - F_c^2)^2]/\Sigma(wF_o^2)\}^{\frac{1}{2}}$, where $w = [\sigma^2(F_o^2) + (0.078p^2 + 15P)^2]^{-1}$ and $P = 0.3333$ maximum of $(0$ or $F_o^2) + 0.6667F_c^2$. The final difference map showed no significant residual electron density. All programs used in the structure refinement are contained in the SHELXL 92[24] package. Final atomic coordinates are given in Table 6.

Additional material available from the Cambridge Crystallographic Data Centre comprises H-atom coordinates, thermal parameters and remaining bond lengths and angles.

References

1 J.-M. Lehn, *Pure Appl. Chem.*, 1980, **52**, 2441; 1977, **49**, 857.
2 D. McDowell and J. Nelson, *Tetrahedron Lett.*, 1988, **29**, 385.
3 J. Jazwinskii, J.-M. Lehn, D. Lillienbaum, R. Ziessel, J. Guilheim and C. Pascard, *J. Chem. Soc., Chem. Commun.*, 1987, 1691.
4 M. G. B. Drew, J. Hunter, D. Marrs and J. Nelson, *J. Chem. Soc., Dalton Trans.*, 1992, 11.
5 M. G. B. Drew, J. Hunter, D. Marrs, J. Nelson and C. Harding, *J. Chem. Soc., Dalton Trans.*, 1992, 3235.
6 C. Harding, V. McKee and J. Nelson, *J. Am. Chem. Soc.*, 1991, **113**, 9684.
7 D. J. Marrs, V. McKee, J. Nelson, Q. Lu and C. J. Harding, *Inorg. Chim. Acta*, 1993, **211**, 195.
8 Q. Lu, V. McKee and J. Nelson, *J. Chem. Soc., Chem. Commun.*, 1994, 649.
9 D. J. Marrs, Ph.D. Thesis, Open University, 1990.
10 D. McDowell, V. McKee and J. Nelson, *Polyhedron*, 1989, **8**, 1143.
11 D. Marrs, N. Martin, V. McKee, M. G. B. Drew and J. Nelson, *Proc. Conf. Chem. Cu and Zn Triads*, Edinburgh, 1992; D. J. Marrs and J. Nelson, unpublished work.
12 V. McKee, M. Dorrity, J. F. Malone, D. Marrs and J. Nelson, *J. Chem. Soc., Chem. Commun.*, 1992, 383.
13 E. C. Alyea, G. Ferguson, M. C. Jennings and Z. Zu, *Polyhedron*, 1990, **9**, 738.
14 Q. Lu, M. McCann and J. Nelson, *J. Inorg. Biochem.*, 1993, **51**, 633.
15 P. L. Burke, J. A. Osborn, M.-T. Youinou, Y. Angus, R. Louis and R. Wiess, *J. Am. Chem. Soc.*, 1981, **103**, 1273; P. K. Coughlin and S. J. Lippard, *J. Am. Chem. Soc.*, 1981, **103**, 3228.
16 J. Nelson, N. Martin, Q. Lu, J. F. Malone, V. McKee and C. J. Harding, in preparation.
17 C. Harding, Q. Lu, V. McKee and J. Nelson, *J. Chem. Soc., Chem. Commun.*, 1993, 1768.
18 C.-L. O'Young, J. C. Dewan, H. R. Lilienthal and S. J. Lippard, *J. Am. Chem. Soc.*, 1978, **100**, 7291.
19 M. G. B. Drew, P. C. Yates, F. S. Esho, J.-T. Grimshaw, A. Lavery, K. P. McKillop, S. M. Nelson and J. Nelson, *J. Chem. Soc., Dalton Trans.*, 1988, 2995; A. Bencini, D. Gatteschi, J. Reedijk and C. Zanchini, *Inorg. Chem.*, 1985, **24**, 207.
20 P. Chaudhuri, I. Karpenstein, M. Winter, M. Lengen, C. Butzlaff, E. Bill, A. X. Trautwein, U. Florke and H.-J. Haupt, *Inorg. Chem.*, 1993, **32**, 888.
21 D. N. Hendrickson and T. Felthouse, *Inorg. Chem.*, 1978, **17**, 444.
22 G. M. Sheldrick, SHELXTL-PC (Version 4.1), Siemens Analytical X-Ray Instruments, Madison, WI 1989.
23 G. M. Sheldrick, SHELXS86, *Acta Crystallogr., Sect. A*, 1990, **46**, 467.
24 G. M. Sheldrick, SHELXL 92, *J. Appl. Crystallogr.*, in preparation.